Nanoimprinted plastic substrates for enhanced surface plasmon resonance imaging detection

Lidija Malic,[1,2] Bo Cui,[2,3] Maryam Tabrizian,[1] and Teodor Veres[2,*]

[1]*Biomedical Engineering Department, McGill University, Montreal, QC, CANADA*
[2]*Industrial Materials Institute, Boucherville, QC, CANADA*
[3]*Currently with the Department of Electrical and Computer Engineering, University of Waterloo, Waterloo, ON, CANADA*
**Teodor.Veres@cnrc-nrc.gc.ca*

Abstract: Periodic nanostructures fabricated by Nanoimprint Litography (NIL) in low-cost plastic substrates and coated with thin gold film were explored for enhanced surface plasmon resonance imaging (SPRi) detection. Rigorous coupled-wave analysis was used to model the SPRi response of these nanostructured surfaces. Two-dimensional nanogratings and nanogrooves were fabricated on Zeonor 1060R™ by NIL and followed by metal deposition. The detection of refractive index changes in the dielectric layer due to bulk medium change, DNA immobilization and DNA hybridization events were monitored using SPRi to assess the corresponding signal amplification. The results indicate target-dependent sensitivity enhancement which is maximized for the detection of biomolecular binding events. The 500 nm period nanogrooves provided a 4 times SPR signal amplification compared to the conventional uniform gold film on SF-11 glass for DNA hybridization detection. Our work demonstrates that the use of nanoimprinted plastic substrates provides a low-cost solution for the SPR-based detection with sensitivity that meets the requirements in practical diagnostic applications.

OCIS codes: (240.6680) Surface Plasmons; (130.6010) Sensors; (050.2770) Gratings; (260.3910) Optics of Metals; (310.6860) Thin films Optical Properties; (120.1880) Detection.

References and links

1. M. E. Stewart, C. R. Anderton, L. B. Thompson, J. Maria, S. K. Gray, J. A. Rogers, and R. G. Nuzzo, "Nanostructured plasmonic sensors," Chem. Rev. **108**(2), 494–521 (2008).
2. A. B. Dahlin, J. O. Tegenfeldt, and F. Höök, "Improving the instrumental resolution of sensors based on localized surface plasmon resonance," Anal. Chem. **78**(13), 4416–4423 (2006).
3. A. J. Haes, and R. P. V. Duyne, "A unified view of propagating and localized surface plasmon resonance biosensors," Anal. Bioanal. Chem. **379**(7-8), 920–930 (2004).
4. E. Hutter, and J. H. Fendler, "Exploitation of localized surface plasmon resonance," Adv. Mater. **16**(19), 1685–1706 (2004).
5. K. M. Byun, S. J. Yoon, D. Kim, and S. J. Kim, "Experimental study of sensitivity enhancement in surface plasmon resonance biosensors by use of periodic metallic nanowires," Opt. Lett. **32**(13), 1902–1904 (2007).
6. L. Malic, B. Cui, T. Veres, and M. Tabrizian, "Enhanced surface plasmon resonance imaging detection of DNA hybridization on periodic gold nanoposts," Opt. Lett. **32**(21), 3092–3094 (2007).
7. K. M. Byun, M. L. Shuler, S. J. Kim, S. J. Yoon, and D. Kim, "Sensitivity Enhancement of Surface Plasmon Resonance Imaging Using Periodic Metallic Nanowires," J. Lightwave Technol. **26**(11), 1472–1478 (2008).
8. K. M. Byun, D. Kim, and S. J. Kim, "Investigation of the profile effect on the sensitivity enhancement of nanowire-mediated localized surface plasmon resonance biosensors," Sens. Act. B. **117**(2), 401–407 (2006).
9. D. Kim, "Effect of resonant localized plasmon coupling on the sensitivity enhancement of nanowire-based surface plasmon resonance biosensors," J. Opt. Soc. Am. A **23**(9), 2307–2314 (2006).
10. C. J. Alleyne, A. G. Kirk, R. C. McPhedran, N.-A. P. Nicorovici, and D. Maystre, "Enhanced SPR sensitivity using periodic metallic structures," Opt. Express **15**(13), 8163–8169 (2007).
11. S. Park, G. Lee, S. H. Song, C. H. Oh, and P. S. Kim, "Resonant coupling of surface plasmons to radiation modes by use of dielectric gratings," Opt. Lett. **28**(20), 1870–1872 (2003).

#115602 - $15.00 USD Received 17 Aug 2009; revised 23 Sep 2009; accepted 24 Sep 2009; published 23 Oct 2009

12. S. Elhadj, G. Singh, and R. F. Saraf, "Optical properties of an immobilized DNA monolayer from 255 to 700 nm," Langmuir **20**(13), 5539–5543 (2004).
13. S. J. Yoon, and D. Kim, "Target dependence of the sensitivity in periodic nanowire-based localized surface plasmon resonance biosensors," J. Opt. Soc. Am. A **25**(3), 725–735 (2008).
14. L. Malic, T. Veres, and M. Tabrizian, "Biochip functionalization using electrowetting-on-dielectric digital microfluidics for surface plasmon resonance imaging detection of DNA hybridization," Biosens. Bioelectron. **24**(7), 2218–2224 (2009).
15. A. W. Peterson, R. J. Heaton, and R. M. Georgiadis, "The effect of surface probe density on DNA hybridization," Nucleic Acids Res. **29**(24), 5163–5168 (2001).

1. Introduction

The use of surface plasmon resonance imaging (SPRi) has emerged in the last few years as a promising alternative to traditional fluorescence-based assays for parallel, real-time, label-free detection of binding interactions in several fields. This is evidenced by the growing number of publications in the fields of medical diagnostics, environmental monitoring, and food safety and security. However the sensitivity of available SPRi instrumentation is limited by small angular shift of the SPR spectrum dip and small fractional reflectivity change, which limits its development as a practical diagnostic tool for clinical applications. The current and future demands of these applications require compact, inexpensive and highly sensitive SPR surfaces. Hence, increasing the sensitivity and improving the bio-interface to generate bigger signals has been an active area of research. For instance, to overcome the sensitivity limitation, nanostructure-based SPR biosensors have drawn tremendous interest in recent years [1–4]. The exploitation of metallic nanostructures allows strong optical coupling of incident light to localized surface plasmons (LSPs). These depend on the nanostructure shape, size, composition and dielectric environment. LSP resonances are also accompanied by electromagnetic field enhancements, which are used for the development of novel transduction mechanisms in surface-enhanced spectroscopies. For conventional SPR and SPRi, the sensitivity enhancement is attributed to strong interactions between LSPs, propagating SPs, and binding biomolecules, which leads to a change in the resonance conditions and consequently to an additional shift of resonance angle and reflectivity [5–9]. Various noble metal nanostructures fabricated on SPR-active thin film of biosensor chip have been used to amplify the SPR signals of prism-coupled (Kretschmann arrangement) SPR instrumentation [5,6]. Recent theoretical and experimental studies have shown that the periodic Au nanostructures, such as nanowires, nanogratings and nanoposts, provide a considerable sensitivity enhancement compared to conventional flat-surface SPR sensor [5–10]. By adding a corrugation to the biosensor interface of prism-coupled SPR sensor, the propagation of the surface plasmon is perturbed, yielding an enhancement of sensitivity [10]. However, high costs associated with conventional fabrication of these substrates via electron beam lithography (EBL) limits their use in practical applications. In this work, periodic metal nanogratings and nanogrooves deposited on nanostructured template fabricated on low-cost plastic substrates are investigated both numerically and experimentally for enhanced SPRi detection of various targets ((i) bulk medium refractive index change due to different salt concentrations in water, (ii) monolayer formation due to DNA immobilization on gold surface, and (iii) biomolecular interactions due to DNA hybridization event).

2. Numerical model

The well-established rigorous coupled wave analysis (RCWA) is successfully employed to model the sensitivity to different target analytes as a function of the nanostructured substrate geometry and corroborate the experimental results [7,11]. For simplicity, the nanostructure-based SPR substrate is represented as an array of 500 and 600 nm period rectangular plastic (n_{zeonor} = 1.53) nanogratings (Fig. 1(a)) or nanogrooves (Fig. 1(b)), 80 and 30 nm in size, respectively. As a comparison, a conventional SPR structure is represented by a plain gold film on SF-11 glass substrate ($n_{SF\text{-}11}$ = 1.765), used and referred to hereafter as the control

#115602 - $15.00 USD Received 17 Aug 2009; revised 23 Sep 2009; accepted 24 Sep 2009; published 23 Oct 2009

(Fig. 1(c)). Both substrates are covered by a 50 nm thick gold layer, which is an optimum value for the planar SPR interface. This represents the experimental conditions, whereas the metal film deposition is performed simultaneously for all substrates.

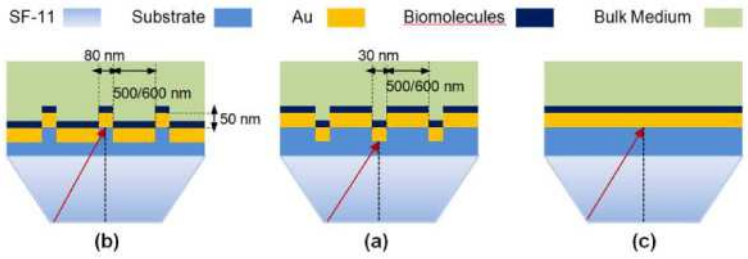

Fig. 1. Schematics of investigated SPR biosensor structures (a) nanogratings (b) nanogrooves (c) conventional planar gold SPR interface (control)

Bulk medium refractive index change due to different salt concentration (C) in water is modeled by changing the refractive index of aqueous solution from 1.333 to 1.363 in 0.01 increments. DNA immobilization event is modeled by adding a homogeneous single-stranded ssDNA monolayer on top of the gold layer using the values from Elhadj et al. provided in Ref [12]. The DNA hybridization event is modeled by changing the refractive index and thickness of the ssDNA monolayer by 5% and 3.5 nm, respectively, to form a double-stranded dsDNA [12]. The simulation is performed by scanning the incidence angle of a transverse magnetic (TM) polarized monochromatic plane wave at 800 nm wavelength with an angular resolution of 0.01°. Calculations were carried out using 100 space harmonics with 1 nm resolution in the grating depth axis and 512 steps per grating period. The sensitivity enhancement factor (*SEF*) is defined as the ratio of resonant angle shift due refractive index change of the dielectric layer ($\Delta n = n_2 - n_1$) in contact with the gold film (bulk medium, ssDNA or dsDNA) of the nanostructured surface (Fig. 1(a) and (b)) to that of control (Fig. 1(c)):

$$SEF = \left| \frac{\Delta\theta_{NSPR}}{\Delta\theta_{SPR}} \right| = \left| \frac{\theta_{NSPR(n_2)} - \theta_{NSPR(n_1)}}{\theta_{SPR(n_2)} - \theta_{SPR(n_1)}} \right|$$

where θ_{NSPR} and θ_{SPR} represent the resonant angle with and without the nanoposts, respectively. Figure 2 shows the calculated SEF for 500 nm and 600 nm period nanogratings and nanogrooves.

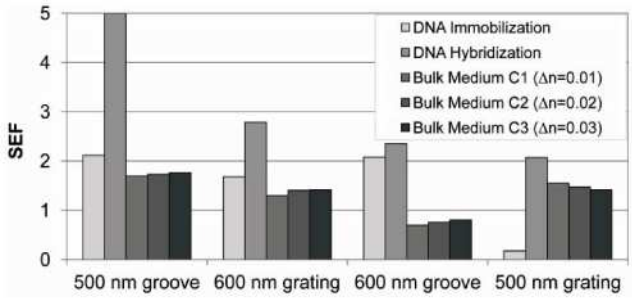

Fig. 2. Numerically obtained SEF that corresponds to different target analyte for SPR substrates with 500 nm and 600 nm period nanogrooves and nanogratings

It is interesting to note that while the nanostructure period and geometry play an important role in the overall performance of the nanostructured plastic surface response, also pronounced is the sensitivity variation due to the target analyte. In fact, it was previously shown using RCWA that the sensitivity is a complex function of an SPR sensor structure as

#115602 - $15.00 USD Received 17 Aug 2009; revised 23 Sep 2009; accepted 24 Sep 2009; published 23 Oct 2009

well as the target itself [13]. Yoon and Kim have developed an analytical model based on effective media in a study involving gold nanowires to show that the target-dependant sensitivity can be attributed to nonlinearity between the resonance conditions and the target refractive index in the plasmon dispersion relation [13]. Herein, the bulk refractive index change has lower effect on the sensitivity enhancement than the reaction involving biomolecule adsorption on the SPR surface. The highest SEF occurs for the DNA hybridization reaction, with a maximum value of 5 for 500 nm period nanogrooves.

3. Substrate fabrication

Nanostructured substrates were replicated in plastic (amorphous cyclo-olefin polymer Zeonor-1060R, Zeon Inc.) from a silicon mould using NIL (EVG, Austria) at a temperature of 170°C and 15 atmosphere pressure for 10 min. The silicon mould containing the inverted nanostructure profile was prepared using EBL (Hitachi S4800, Japan) on 240 nm thick Zep-520A resist. The exposure was done using 30 kV acceleration voltage and 500 pA beam current, followed by the development in ZED-N50 developer. The thermally grown SiO_2 was etched using reactive ion etching (RIE, PlasmaLab 80 Plus, Oxford Instruments, UK) for 3 min with 20 sccm CHF_3 at 100 W and 10 mTorr. The remaining Zep-520A resist was subsequently stripped using oxygen plasma (20 sccm O_2) at 100 W and 100 mTorr for 1 min. After NIL, 50 nm thick gold film was deposited on the imprinted substrates by sputtering (Kurt-J-Lesker CMS, USA) to ensure conformal coating. Figure 3 shows the scanning electron microscope (SEM, Hitachi S4700, Japan) and atomic force microscope (AFM, Veeco, USA) images of the fabricated 500 nm period nanogratings and nanogrooves. Both 500 nm and 600 nm period structures had widths of 80±4.7 nm and 30±3.9 nm, respectively. The height (45 nm) and the period were found to be of excellent uniformity with 2.8% and 3.4% variation, respectively.

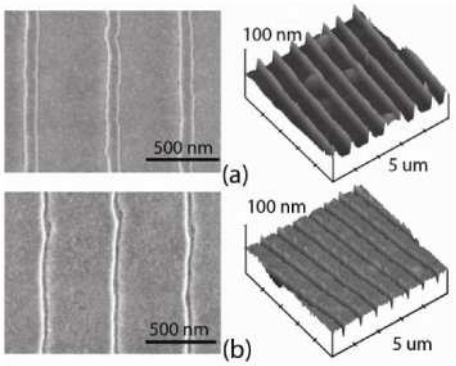

Fig. 3. SEM and AFM images of (a) 500 nm period nanogratings and (b) 500 nm period nanogrooves.

4. Experimental SPRi measurements

All plasmon and kinetic curves were obtained using scanning-angle SPRi instrument (Fig. 4) equipped with 800 nm LED source and a CCD camera (model SPRi-Lab+ , GenOptics, France). The kinetic measurements for each sample were performed near the resonance at an angle which corresponds to the maximum value of the slope in the reflectivity curve for maximum sensitivity. Four points comprising 100 µm spots were measured in parallel on each sample and the average value is reported for three experimental runs on fresh new substrates.

#115602 - $15.00 USD Received 17 Aug 2009; revised 23 Sep 2009; accepted 24 Sep 2009; published 23 Oct 2009

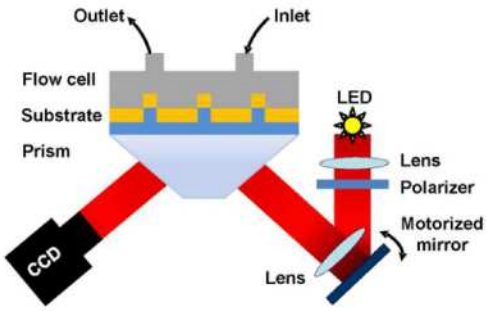

Fig. 4. Schematic representation of SPRi optical setup

The resonant angle change due to refractive index change of bulk medium was monitored for different NaCl salt (Sigma-Aldrich, St. Louis, Mo, USA) concentrations (250 mM (C1), 500 mM (C2) and 1 M (C3)) in ultra pure water (UPW). The experimentally obtained SEF due to the bulk medium refractive index change is compared to the numerically obtained values in Fig. 5. In general, the experimentally obtained values agree well with the numerical calculations with the exception of 250 mM NaCl salt concentration (C1). At this value, the numerical calculation underestimates the performance of the nanostructured sensor. This is due to the lower model value taken for the initial change of the refractive index of water following the first addition of salt (C1).

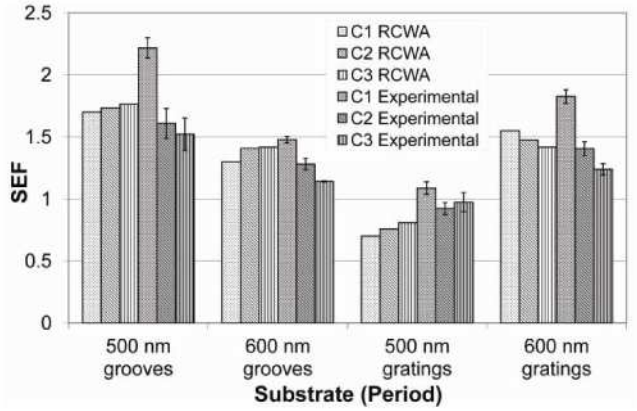

Fig. 5. Comparison of experimentally and numerically obtained SEF for different salt concentrations in water (different bulk medium refractive index change).

Surface functionalization of substrates was performed by immobilizing 1 μM 20-mer oligonucleotide probe sequence (5′-/HS-C6/-GCGGCATGAACCGGAGGCCC-3′, Integrated DNA Technologies, Coralville, IA) with thiol modification at the 5′-end in 1M potassium phosphate dibasic solution (1 M KH_2PO_4, pH 8.9 Sigma-Aldrich, St. Louis, USA) for 120 min, based on previously optimized immobilization conditions on flat gold surface [14]. SPRi kinetic signal was obtained first for immobilization solution (1 M KH_2PO_4), followed by immobilization signal. Following immobilization, substrates were treated with 20 mM Heptadecafluoro-1-decanethiol (>99%, Fluka, Sigma-Aldrich, St. Louis, USA) in ethanol for 10 min to render the probes highly accessible to the target while preventing unspecific target-adsorption to the gold surface [14]. DNA hybridization experiments were carried out using 20-mer oligonucleotide target sequence complementary to the immobilized probe. Hybridization kinetic curves were monitored by obtaining a baseline signal for hybridization buffer (1 M NaCl in Tris-EDTA (TE) buffer solution, pH 8.0, Sigma-Aldrich, St. Louis, USA). This was followed by hybridization signal for which 250 nM target was injected into

#115602 - $15.00 USD Received 17 Aug 2009; revised 23 Sep 2009; accepted 24 Sep 2009; published 23 Oct 2009

the flow cell allowing the target to bind to the immobilized probe for 10 min to yield sufficient refractive index change while minimizing the reaction time. Finally, the substrates were washed with buffer and the difference in the reflected intensity was computed by the difference between the initial and final buffer injections. The SPRi detection limit for DNA hybridization was obtained by injecting sequentially incremental DNA target concentrations from 100 pM to 100 nM every 8 minutes. The SPRi kinetic curves of nanostructured plastic substrates for different binding reactions are shown in Fig. 6.

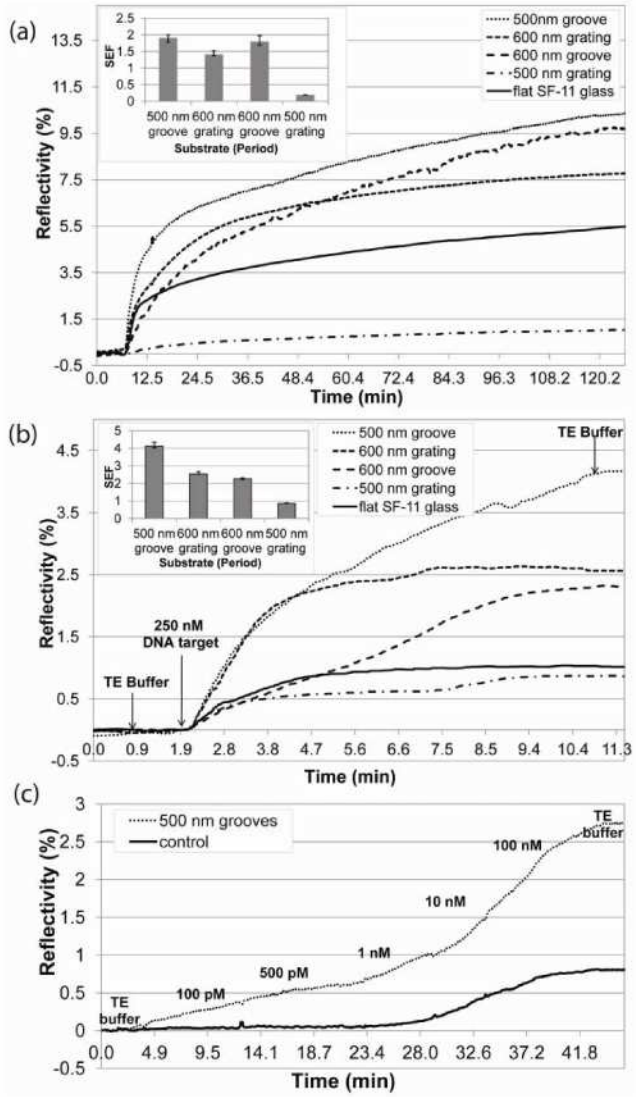

Fig. 6. SPRi Kinetic curves showing binding reactions on gold-coated nanostructured plastic substrates for (a) 2 hrs immobilization of 1 μM DNA probe; (b) 10 min hybridization of 250 nM DNA target; (c) DNA hybridization concentration gradient comparing the detection limits of nanogroove sensor surface to that of control.

To enable qualitative assessment of the effect of nanostructured surface on SPR signal amplification, the experimental SEF (inset of Fig. 6(a) and (b)) which describes the ratio of the change in reflected intensity due to DNA immobilization and hybridization on nanostructured surface to that of control is included. Figure 6(a) and (b) shows DNA

#115602 - $15.00 USD Received 17 Aug 2009; revised 23 Sep 2009; accepted 24 Sep 2009; published 23 Oct 2009

immobilization on the gold surface of the substrates and subsequent DNA hybridization reaction. In both cases, 500 nm period nanogrooves yield highest SEF corresponding to 4.13 and 1.91, which is in close agreement with the numerically estimated signal amplification (Fig. 2). The small discrepancy between the two is expected, as the refractive index change in the numerical model overestimates the experimental refractive index change induced by DNA immobilization and hybridization reactions, for unsaturated surface. The 500 nm period nanogratings had 2.4 times less efficient performance for DNA hybridization reaction than predicted by the numerical model. This was due to the curve broadening at this period which caused uncertainty in values of the resonance peak and also resulted in lower change of reflected intensity. The target induced SEF variation becomes apparent by comparing the results depicted in Fig. 6(a) and Fig. 6(b). In the case of DNA hybridization, the enhancement is up to 2.16 times higher than the enhancement for the DNA immobilization. This suggests that the functionalized surface of the nanostructured plastic substrate provides higher sensitivity for biomolecule binding reactions compared to the bare gold surface. This can be explained in terms of the electromagnetic field enhancement experienced by the nanostructured surface in the absence / presence of immobilized biomolecules. As previously mentioned, the field enhancement provided by the nanostructures is a complex function of the nanostructure composition, dimension, geometry and the dielectric (biomolecular) environment. In our case, the addition of the monolayer at the surface of the nanostructured substrates, as demonstrated by the results obtained for the 500 nm period grooves, created a maximum electromagnetic field enhancement in the vicinity of the monolayer, which was larger than the field enhancement experienced by the bare gold surface. This resulted in increased signal amplification for the hybridization event, involving the creation of the duplex within the monolayer, as compared to the monolayer assembly on bare gold surface. It is also interesting to note that for 500 nm nanogrooves, the enhancement is higher for smaller refractive index changes, which is represented by lower concentrations of the DNA target (Fig. 6(c)). The experimental limit of detection for this configuration was found to be 100 pM, compared to ~5 nM for flat SF-11 substrate.

5. Conclusion

In this paper, we have shown that low-cost nanostructured plastic substrates can be used to enhance the sensitivity of conventional SPR imaging. We have demonstrated both numerically and experimentally that due to the increased surface binding area and the excitation and coupling of localized and bulk SPs provided by the nanogratings and nanogrooves, the SPR signal can be amplified up to four times in only 10 min of DNA hybridization, as was the case for 30 nm wide nanogrooves with 500 nm period. While the assay was designed for demonstrating the nanostructure-based signal enhancement using well-known thiol-based chemistry [15], the obtained sensitivity improvement is significant in comparison with a conventional SPRi detection, with potential for future diagnostic applications. Further optimization of the initial gold film thickness and the nanostructure size and periodicity are required while considering the appropriate surface modification for a particular application.

Acknowledgments

The authors thank le Fonds québécois de la recherche sur la nature et les technologies (FQRNT) for the scholarship, FQRNT-team grant, FQRNT-Centre for Biorecognition and Biosensors, Genome Canada, and the Industrial Materials Institute of the National Research Council of Canada for their financial support.

#115602 - $15.00 USD Received 17 Aug 2009; revised 23 Sep 2009; accepted 24 Sep 2009; published 23 Oct 2009